

The pyroxenite-diamond connection

E.S. Kiseeva^{1*}, B.J. Wood¹, S. Ghosh², T. Stachel³



doi: 10.7185/geochemlet.1601

Abstract

Pieces of the Earth's mantle occurring either as tectonic fragments or xenoliths in volcanic rocks are dominantly peridotites, assemblages of olivine, ortho- and clinopyroxene with minor garnet and/or spinel. They frequently contain pyroxene-rich inclusions which have compositions intermediate between peridotite and basalt. These pyroxenites typically contain varying amounts of more iron-rich (than peridotite) clinopyroxene, orthopyroxene, garnet and/or spinel and are commonly compositionally layered. Surprisingly, despite their subordinate abundance in mantle fragments, pyroxenitic compositions appear to be the dominant sources of majoritic garnet inclusions in diamonds, the principal window into the mineralogy of the deep upper mantle and the transition zone (Kiseeva *et al.*, 2013a). In this study we show that the pyroxenite-diamond association is a consequence of the interaction between basaltic and peridotitic compositions in the presence of carbonate melt and that layering of the pyroxenites is a natural consequence of this interaction. Reduction of carbonate to carbon at high pressures is responsible for the genetic connection between pyroxenite and diamond and the abundance of pyroxenitic inclusions reflects this connection rather than a high abundance of this rock type in the mantle.

Received 8 July 2015 | Accepted 17 September 2015 | Published 15 October 2015

Letter

Between 8–15 GPa, with increasing pressure the orthopyroxene and clinopyroxene of peridotite dissolve into garnet through the peridotitic “majorite” substitution: $2\text{Al}^{3+} = \text{Si}^{4+} + \text{M}^{2+}$, where M^{2+} represents divalent Mg, Fe, Ca and Mn (Fig. 1). In the transition zone (410–660 km depth) “peridotite” thus becomes a biminerally composed of majorite plus a high pressure polymorph of $(\text{Mg,Fe})_2\text{SiO}_4$ (wadsleyite or ringwoodite). Under the same conditions basalt initially transforms to eclogite (garnet plus clinopyroxene) and then with increasing pressure the clinopyroxene dissolves into the garnet through a combination of the peridotitic

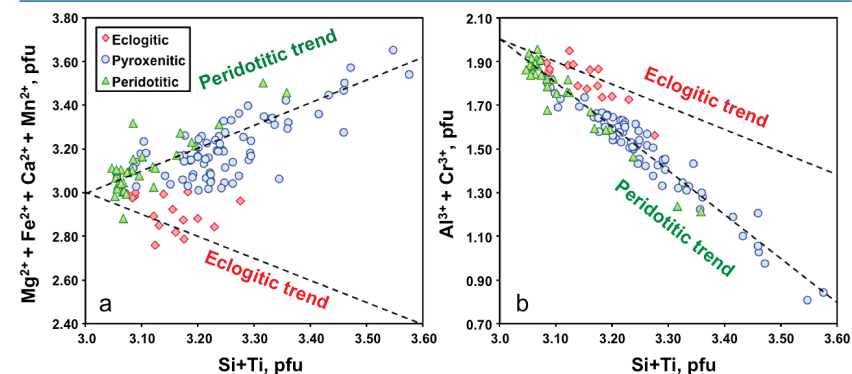


Figure 1 Compositions of 16 eclogitic, 75 pyroxenitic and 32 peridotitic majorite inclusions in natural diamonds as functions of (Si + Ti) pfu (per formula unit), showing (dashed lines) the theoretical “peridotitic” and “eclogitic” substitutions discussed in the text (after Kiseeva *et al.*, 2013a).

Figure 2a shows the compositions of majoritic inclusions, MORB, peridotites and pyroxenites. Garnets of pyroxenitic affinity are higher in MgO and lower in Al_2O_3 than those of eclogitic affinity. Using geobarometers based on the Si content of majoritic garnet (Collerson *et al.*, 2010; Beyer, 2015), these inclusions were formed at pressures of 7–18 GPa with values above 15 GPa being rare. At these pressures clinopyroxene should coexist with the garnet in some, but not all, pyroxenitic compositions, an inference which is supported by general compositional differences between majorite garnet and bulk MORB and pyroxenite

1. Department of Earth Sciences, University of Oxford, Oxford OX1 3AN, UK
* Corresponding author (email: kate.kiseeva@earth.ox.ac.uk)
2. Institute of Geochemistry and Petrology Department of Earth Sciences, ETH Zürich, 8092 Zürich, Switzerland. Current address: Department of Geology & Geophysics, Indian Institute of Technology, Kharagpur, 721302 Kharagpur, India
3. Department of Earth and Atmospheric Sciences, University of Alberta, Edmonton, AB T6G 2E3, Canada



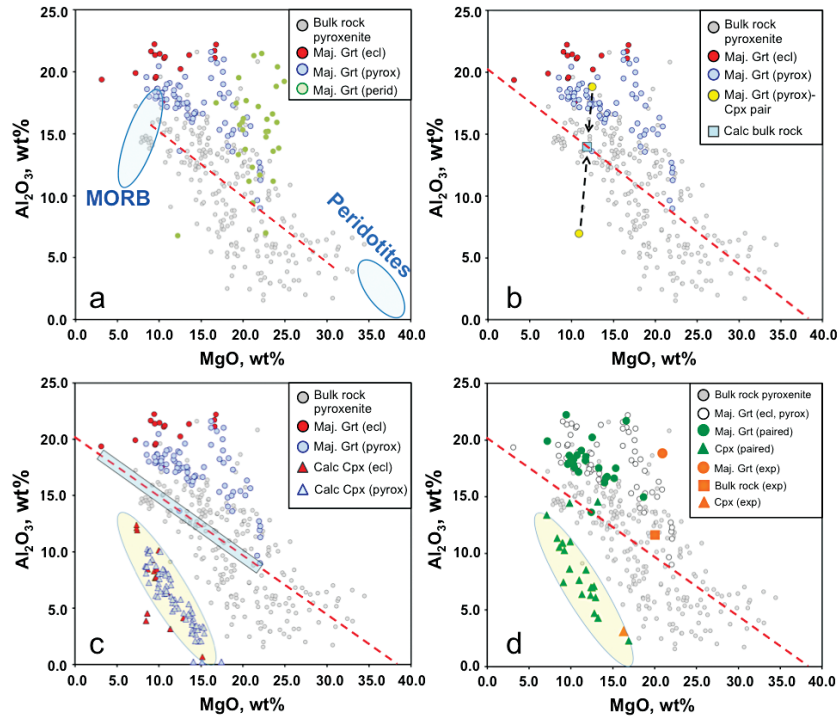


Figure 2 Bulk compositions of natural pyroxenites (grey circles) plotted in $MgO-Al_2O_3$ compositional space. Dashed red line shows the regression line for all the pyroxenites. (a) Compositions of majoritic inclusions in diamonds of eclogitic (red), pyroxenitic (blue) and peridotitic (light green) affinities. Fields of bulk rock peridotite and MORB are shown as blue ovals. (b) Tie line between a majoritic garnet and calculated coexisting clinopyroxene (Cpx; see text for details). A possible bulk rock composition for this pair was placed on the red regression line. (c) Population of natural majoritic garnets and reconstructed clinopyroxene compositions. Field of Cpx compositions is shown with the yellow oval. Note wide range of potential bulk (pyroxenitic) source rock compositions. Placement of the latter around the regression line is meant only to be indicative. (d) Majoritic inclusions in diamonds (green circles) which coexist with clinopyroxene(s) (green triangles) within the same diamond. The range of observed natural clinopyroxene compositions occupy the area predicted by our modelling. Orange circles show the bulk composition and the majorite-clinopyroxene pair which crystallised in an experimental run at 15 GPa and 2150 °C.

(Fig. 2a and Supplementary Information). Instances of 2 phase (clinopyroxene-garnet) assemblages in the same diamond are, however, rare, which may reflect a specific connection between the diamond-forming process discussed below and garnet. Nevertheless, we began by estimating the compositions of the clinopyroxenes with which the observed majoritic garnets should coexist. We used

around 50 high-pressure experiments on garnet-clinopyroxene pairs as a basis of our estimates (Supplementary Information). These experiments give us a Na partitioning expression:

$$Na_{Cpx}^{6ox} = \frac{Na_{Grt}^{12ox}}{0.262 + 0.0241P - 0.00014T} \quad \text{Eq. 1}$$

where P is in GPa and T is in K. In Equation 1, the Na contents of clinopyroxene (Cpx) and garnet (Grt) are cation values on 6 and 12 oxygen bases, respectively. We then assumed that, at these high pressures, tetrahedral Al in clinopyroxene is low (0.01 cations per formula unit) and that octahedral Al on the M1 site is Na plus octahedral Al coupled to tetrahedral Al (*i.e.* $NaAlSi_2O_6$ and $CaAl_2SiO_6$ substitutions respectively). We calculated the Ca content of the M2 clinopyroxene site by assuming that Na+Ca on this site is 0.95 cations per formula unit, thus allowing 0.05 of (Mg+Fe) on the large M2 site. We then assumed that Si is 2.0 minus tetrahedral Al and that Mg+Fe fill the remaining M1 and M2 sites. The ratio $Mg/(Mg+Fe)_{Cpx}$ was obtained from the garnet composition using our experimental observations which yield:

$$K_d^{Grt-Cpx} = \frac{[Fe/Mg]_{Grt}}{[Fe/Mg]_{Cpx}} \approx 2 \quad \text{Eq. 2}$$

In this study we use a database of 16 eclogitic, 75 pyroxenitic and 32 peridotitic majorites reported in the literature (Fig. 2a) and calculate a clinopyroxene composition for each one, shown in each one, shown in Figure 2b.

Figures 2a,b,c show bulk rock compositions of natural pyroxenites (*e.g.*, Hirschmann and Stolper, 1996) together with observed compositions of garnet inclusions in diamond and those of clinopyroxenes calculated to coexist with these garnets. The lines between garnet and clinopyroxene cross the pyroxenite field and, for the “pyroxenitic” inclusions cover almost the entire range of compositions of pyroxenites (Fig. 2c and Supplementary Information). For simplicity we have placed a putative “bulk” composition for the source of each inclusion on the red regression line through the pyroxenite compositional data of Hirschmann and Stolper (1996). Note that the recalculated clinopyroxenes occupy a fairly narrow field highlighted in Figure 2c by a yellow oval.

As mentioned above, inclusions of majoritic garnet and clinopyroxene in the same diamond are extremely rare, but nevertheless the few occurrences available enable us to test our calculation method (Fig. 2d). In Figure 2d we compare our field of calculated clinopyroxene compositions with the observed compositions of clinopyroxenes coexisting with garnet in the same diamond. As can be seen, the agreement is excellent. Similarly, in Figure 2d we show the results of an experiment in which a pyroxenitic bulk composition was reacted at 15 GPa and 2150 °C. Despite the extreme temperature, used to enhance reaction rates, the composition of clinopyroxene coexisting with garnet can also be seen to be in excellent agreement with our calculation approach.



The large number of pyroxenites found in ophiolitic complexes, alpine massifs, and as mantle xenoliths (Hirschmann and Stolper, 1996; Fig. 2a) suggest that there are common and widespread mechanisms for the formation of lithologies intermediate between a typical basalt (or eclogite) and peridotite. Given the wide range of compositions and mineralogies found in such “pyroxenites” it is likely that more than one mechanism applies (Downes, 2007). However, the predominance of sublithospheric garnet inclusions of pyroxenitic affinity (Kiseeva *et al.*, 2013a) strongly suggests that one important and widespread mechanism involves carbon. Since diamond is inert, the most plausible origin of the association is through interaction between eclogite and peridotite in the presence of carbonated melt or fluid.

In order to investigate the possible formation of pyroxenite through the interaction of carbonated eclogite with peridotite we performed high-pressure sandwich experiments in a piston-cylinder apparatus. Model quartz-eclogite and peridotite compositions in the system CaO-MgO-Al₂O₃-SiO₂ (reduced in CaO content to take account of added carbonate) were mixed with ~5 % of CaCO₃ and loaded on top of one another in a 3 mm Pt capsule. The capsule was welded shut and the experiments performed at 3 GPa and 1350 °C for between 1.5 and 8 hours (Supplementary Information). Under these conditions a SiO₂-poor carbonate melt develops from the CaCO₃ introduced in the starting materials and enhances the rates of reaction between the two principal lithologies.

The experiments simulate a sharp compositional boundary between peridotite and basalt (coesite-eclogite at 3 GPa), analogous to the situation in subducted lithosphere having veins and lenses of basaltic composition dispersed in peridotite (Allègre and Turcotte, 1986). In such cases, according to Korzhinskii (1959), we would expect development of high variance assemblages, typically monomineralic zones, controlled by diffusion of major elements between the two components. Figure 3 shows a schematic (simplified) chemical potential diagram in $\mu_{\text{CaO}}-\mu_{\text{MgO}}$ space which exhibits how mineralogical banding should develop between coesite-eclogite and peridotite.

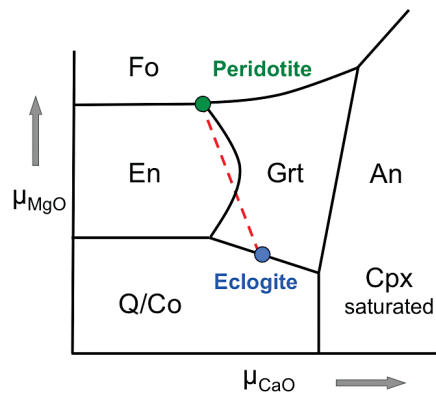


Figure 3 Chemical potential diagram (at fixed pressure and temperature) showing stabilities of phases coexisting with clinopyroxene. Curvature of garnet field boundaries is due to changing composition on passing from eclogite to peridotite (see text). Interaction between eclogite and peridotite will lead to gradients in chemical potentials of MgO and CaO (red dashed line) and layers of orthopyroxene next to peridotite and garnet next to eclogite. Fo – forsterite, En – orthopyroxene, Q/Co – quartz/coesite, Grt – garnet, An – anorthite, Cpx – clinopyroxene.

Both rocks contain clinopyroxene and garnet, but the excess SiO₂ in the eclogite should react with the peridotite to form a layer of orthopyroxene (\pm clinopyroxene) next to the peridotite and a layer enriched in garnet and without coesite next to the eclogite. The garnet should become more Mg-rich as we pass from eclogite to peridotite and we have represented this predicted change with curved boundaries to the garnet field. Figure 4 shows back-scattered electron images of the products of experiment Sa2-1 which generated the predicted monomineralic layers between eclogite and peridotite. As predicted, after 8 hours of reaction at 1350 °C, garnet composition changes progressively from 22.9 wt. % MgO, 8.8 wt. % CaO in the eclogite layer to 25.1 wt. % MgO, 7.0 wt. % CaO in the garnet layer to 27.0 wt. % MgO, 6.1 wt. % CaO in the peridotite. These phase compositions, in an idealised Fe-free system are consistent with those found in lherzolites and eclogites. The model sandwich experiments demonstrate, therefore, that zoned garnet pyroxenites may be formed as a result of a wall-rock reaction between silica-saturated, carbonated eclogite and silica-undersaturated peridotite.

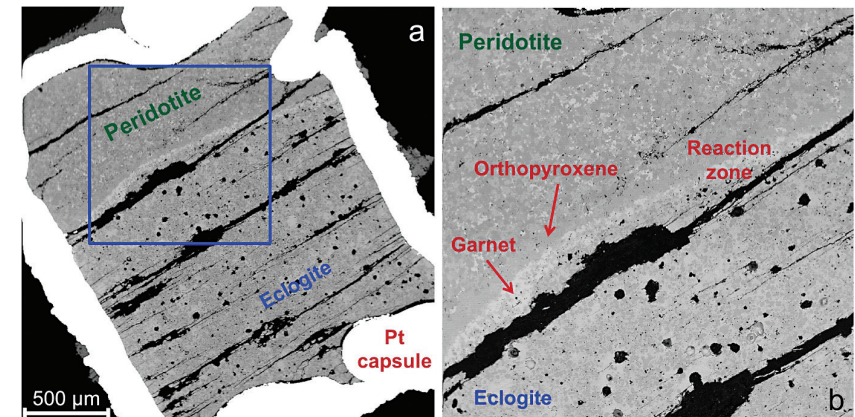


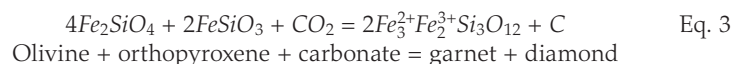
Figure 4 Back-scattered electron images of SA2-1 run products. The experimental conditions are 3 GPa and 1350 °C. Panel (b) shows an enlarged area from panel (a). Orthopyroxene (on the peridotite side) and garnet (on the eclogite-side) are formed within the reaction zone between carbonated eclogite and peridotite.

In the Beni Bousera peridotite massif of Morocco there are frequent veins and lenses of pyroxenite, with or without garnet. That these rocks have been subjected to high pressure (>4.5 GPa) is evidenced by the presence in the pyroxenites of graphite pseudomorphs after diamond (Pearson *et al.*, 1993). Boundaries between pyroxenite and peridotite are generally sharp and pyroxenite veins are often layered with margins of orthopyroxenite or websterite, consistent with Figure 3 and our experiments. The layering has previously been recognised as likely due to interaction between melts and peridotite, and the association



with carbon is consistent with our hypothesis of a connection between carbon and high pressure pyroxenite formation. In this case the carbon has $\delta^{13}\text{C}$ of -16 to -28 per mil, consistent with subducted carbon and the pyroxenites have $\delta^{18}\text{O}$ of +4.9 to 9.3 per mil suggesting an origin as altered oceanic crust. Trace element patterns of websteritic garnet inclusions in diamonds also suggest a mafic precursor source, most likely subducted heterogeneous oceanic crust (Aulbach *et al.*, 2002).

Estimates of the amounts of carbonate subducted into the mantle range from 2.4 to 4.8×10^{13} g of C per year (Dasgupta and Hirschmann, 2010) and numerous studies have indicated that most carbonate survives this process, carrying a characteristic isotopic signature into the deeper mantle (*e.g.*, Kerrick and Connolly, 2001; Yaxley and Brey, 2004). Based initially on density considerations and later on oxygen thermobarometry of garnet peridotites, however, Wood *et al.* (1990, 1996) calculated that carbonate would be unstable in the mantle at depths greater than 140-150 km and would oxidise Fe^{2+} into Fe^{3+} , the latter dissolving into garnet in reactions similar to:



Measurements of $\text{Fe}^{3+}/\text{Fe}^{2+}$ ratios in garnets from the deeper parts of the continental lithosphere (*e.g.*, Woodland and Koch, 2003) support this hypothesis of increasing stability of diamond relative to carbonate with increasing depth. We also found direct evidence of diamond growing in carbonate in an experiment performed on carbonated eclogite at 13 GPa and 1400 °C (Kiseeva *et al.*, 2013b). Similarly, Stagno *et al.* (2013) have shown experimentally that, in normal mantle, carbonate is replaced by diamond and Fe^{3+} -bearing garnet at depths below ~160 km further confirming the validity of our model.

Our experimentally-tested model of the formation of inclusions in diamonds of pyroxenitic affinity therefore follows reaction between eclogite and peridotite in the presence of subducted carbonate to produce garnet-pyroxenite. This is followed by dissolution of pyroxene components into the garnet via the majorite substitution at pressures above ~7 GPa which shifts garnet composition into the general field of pyroxenite (Fig. 2a). The intimate association of C and garnet-bearing pyroxenite culminates with the breakdown of carbonate to diamond plus Fe^{3+} , the latter dissolving in the majoritic garnet. The preponderance of garnet inclusions over those of clinopyroxene may be explained by a combination of the shift of garnet composition into the pyroxenite field with increasing pressure (Fig. 2a) and the potential bias introduced by the diamond-garnet connection described above. The inheritance of shallow crustal signatures observed in sublithospheric pyroxenitic inclusion assemblages (*e.g.*, negative Eu anomalies at elevated MREE-HREE_N; Tappert *et al.*, 2005) and elevated $\delta^{18}\text{O}$ signatures (Ickert *et al.*, 2015) are predictable outcomes of our model. We conclude that the high relative abundance of “pyroxenitic” garnets as inclusions in diamonds

is a consequence of the genetic relationship between carbon and pyroxenite-formation rather than an indication of the high abundance of pyroxenite in the transition zone.

Acknowledgements

We thank Marc Hirschmann and Dante Canil for thorough and constructive reviews. We acknowledge support from European Research Council grant 267764 to BJW and the NERC grant NE/L010828/1 to ESK.

Editor: Bruce Watson

Additional Information

Supplementary Information accompanies this letter at www.geochemicalperspectivesletters.org/article1601



This work is distributed under the Creative Commons Attribution 4.0 License, which permits unrestricted use, distribution, and reproduction in any medium, provided the original author and source are credited. Additional information is available at <http://www.geochemicalperspectivesletters.org/copyright-and-permissions>.

Cite this letter as: Kiseeva, E.S., Wood, B.J., Ghosh, S., Stachel, T. (2016) The pyroxenite-diamond connection. *Geochem. Persp. Let.* 2, 1-9.

References

- ALLÈGRE, C.J., TURCOTTE, D.L. (1986) Implications of a 2-component marble-cake mantle. *Nature* 323, 123-127.
- ANDERSON, D.L., BASS, J.D. (1986) Transition region of the Earth's upper mantle. *Nature* 320, 321-328.
- AULBACH, S., STACHEL, T., VILJOEN, K.S., BREY, G.P., HARRIS, J.W. (2002) Eclogitic and websteritic diamond sources beneath the Limpopo Belt - is slab-melting the link? *Contributions to Mineralogy and Petrology* 143, 56-70.
- BEYER, C. (2015) Geobarometry, phase relations and elasticity of eclogite under conditions of Earth's upper mantle. *PhD thesis*, University of Bayreuth, Interdisciplinary Institutions, 217pp.
- COLLERSON, K.D., WILLIAMS, Q., KAMBER, B.S., OMORI, S., ARAL, H., OHTANI, E. (2010) Majoritic garnet: a new approach to pressure estimation of shock events in meteorites and the encapsulation of sub-lithospheric inclusions in diamond. *Geochimica et Cosmochimica Acta* 74, 5939-5957.
- DASGUPTA, R., HIRSCHMANN, M.M. (2010) The deep carbon cycle and melting in Earth's interior. *Earth and Planetary Science Letters* 298, 1-13.
- DOWNES, H. (2007) Origin and significance of spinel and garnet pyroxenites in the shallow lithospheric mantle: Ultramafic massifs in orogenic belts in Western Europe and NW Africa. *Lithos* 99, 1-24.
- HIRSCHMANN, M.M., STOLPER, E.M. (1996) A possible role for garnet pyroxenite in the origin of the “garnet signature” in MORB. *Contributions to Mineralogy and Petrology* 124, 185-208.



- ICKERT, R.B., STACHEL, T., STERN, R.A., HARRIS, J.W. (2015) Extreme ^{18}O -enrichment in majorite constrains a crustal origin of transition zone diamonds. *Geochemical Perspectives Letters* 1, 65-74.
- KERRICK, D.M., CONNOLLY, J.A.D. (2001) Metamorphic devolatilization of subducted oceanic metabasalts: implications for seismicity, arc magmatism and volatile recycling. *Earth and Planetary Science Letters* 189, 19-29.
- KISEEVA, E.S., YAXLEY, G.M., STEPANOV, A.S., TKALCIC, H., LITASOV, K.D., KAMENETSKY, V.S. (2013a) Metapyroxenite in the mantle transition zone revealed from majorite inclusions in diamonds. *Geology* 41, 883-886.
- KISEEVA, E.S., LITASOV, K.D., YAXLEY, G.M., OHTANI, E., KAMENETSKY, V.S. (2013b) Melting and phase relations of carbonated eclogite at 9–21 GPa and the petrogenesis of alkali-rich melts in the deep mantle. *Journal of Petrology* 54, 1555-1583.
- KORZHINSKII, D.S. (1959) Physicochemical basis of the analysis of the paragenesis of minerals. Translated from Russian. Consultants Bureau, New York. 142pp.
- PEARSON, D.G., DAVIES, G.R., NIXON, P.H. (1993) Geochemical constraints on the petrogenesis of diamond facies pyroxenites from the Beni Bousera peridotite massif, North Morocco. *Journal of Petrology* 34, 125-172.
- STAGNO, V., OJWANG, D.O., MCCAMMON, C.A., FROST, D.J. (2013) The oxidation state of the mantle and the extraction of carbon from Earth's interior. *Nature* 493, 84-90.
- TAPPERT, R., STACHEL, T., HARRIS, J.W., MUEHLENBACHS, K., LUDWIG, T., BREY, G.P. (2005) Subducting oceanic crust: the source of deep diamonds. *Geology* 33, 565-568.
- WOOD, B.J., BRYNDZIA, L.T., JOHNSON, K.E. (1990) Mantle oxidation state and its relationship to tectonic environment and fluid speciation. *Science* 248, 337-345.
- WOOD, B.J., PAWLEY, A., FROST, D.R. (1996) Water and carbon in the Earth's mantle. *Philosophical Transactions of the Royal Society of London Series A-Mathematical Physical and Engineering Sciences* 354, 1495-1511.
- WOODLAND, A.B., KOCH, M. (2003) Variation in oxygen fugacity with depth in the upper mantle beneath the Kaapvaal craton, Southern Africa. *Earth and Planetary Science Letters* 214, 295-310.
- YAXLEY, G.M., BREY, G.P. (2004) Phase relations of carbonate-bearing eclogite assemblages from 2.5 to 5.5 GPa: implications for petrogenesis of carbonatites. *Contributions to Mineralogy and Petrology* 146, 606-619.

The pyroxenite-diamond connection

E.S. Kiseeva^{1*}, B.J. Wood¹, S. Ghosh², T. Stachel³

Supplementary Information

The Supplementary Information includes:

- Pyroxenite compositions
- Trace element compositions of majoritic inclusions in diamonds
- Measured and calculated clinopyroxene compositions
- Pressure estimates for the majoritic inclusions in diamond
- Figures S-1 to S-5
- Tables S-1 and S-2
- Supplementary Information References

Pyroxenite compositions

In Figure 2 of the paper we define the compositional space occupied by peridotites, eclogites, pyroxenites and diamond inclusions solely in terms of a plot of bulk MgO versus Al_2O_3 . We show that pyroxenites are intermediate between peridotite and MORB in $\text{MgO}-\text{Al}_2\text{O}_3$ space. Supplementary Figure S-1a-d adds data for CaO, FeO, SiO_2 and Na_2O and shows that many of the majoritic inclusions in diamonds are themselves of broadly pyroxenitic composition even in the absence of clinopyroxene. When we add different amounts of calculated equilibrium clinopyroxene (see tie lines) a large fraction of the pyroxenite field is covered by the 2-phase assemblages.

1. Department of Earth Sciences, University of Oxford, Oxford OX1 3AN, UK

* Corresponding author (email: kate.kiseeva@earth.ox.ac.uk)

2. Institute of Geochemistry and Petrology Department of Earth Sciences, ETH Zürich, 8092 Zürich, Switzerland. Current address: Department of Geology & Geophysics, Indian Institute of Technology, Kharagpur, 721302 Kharagpur, India

3. Department of Earth and Atmospheric Sciences, University of Alberta, Edmonton, AB T6G 2E3, Canada



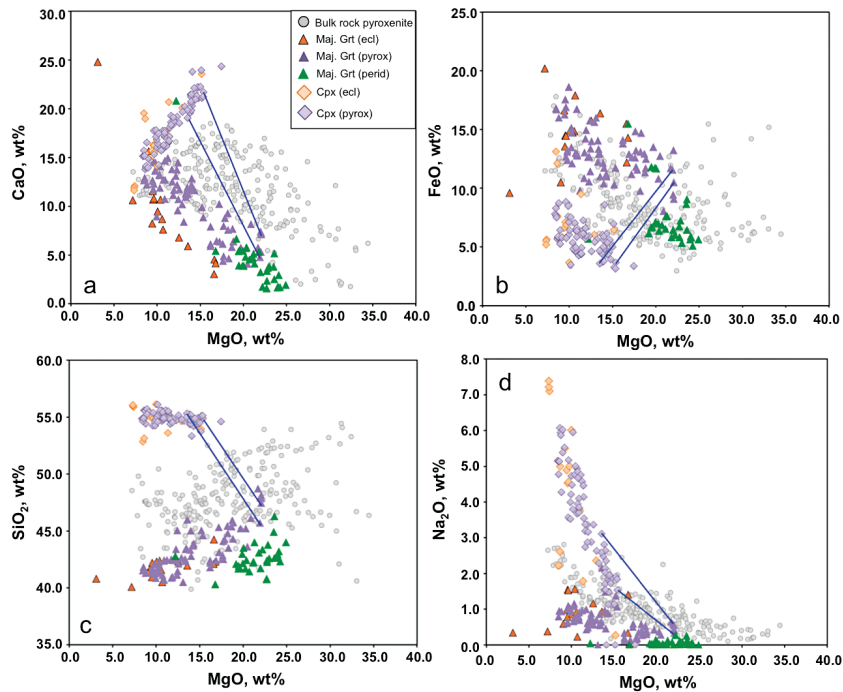


Figure S-1 Bulk rock compositions of natural pyroxenites (grey circles), majoritic inclusions in diamonds of eclogitic (orange triangles), pyroxenitic (purple triangles) and peridotitic (green triangles) affinities and reconstructed clinopyroxene compositions of eclogitic (orange diamonds) and pyroxenitic (purple diamonds) affinities. Blue lines represent selected tie lines between natural majoritic garnets and reconstructed clinopyroxenes.

Trace element compositions of majoritic inclusions in diamonds

In Figures S-2 and S-3 we show the few available data in the literature on the REE, LILE and HFSE contents of majoritic diamond inclusions (Wilding, 1990; Moore *et al.*, 1991; Hutchinson, 1997; Stachel and Harris, 1997; Stachel *et al.*, 1998a,b; Wang *et al.*, 2000; Kaminsky *et al.*, 2001; Pokhilenko *et al.*, 2001; Davies *et al.*, 2003; Pokhilenko *et al.*, 2004; Tappert *et al.*, 2005; Bulanova *et al.*, 2010). As can be seen, despite the evident scatter all the peridotitic majorites are significantly more depleted in LILE, HFSE and REE than pyroxenitic majorites. According to our model of basalt-peridotite interaction, the pyroxenites inherit large fractions of these trace elements from their basaltic precursors.

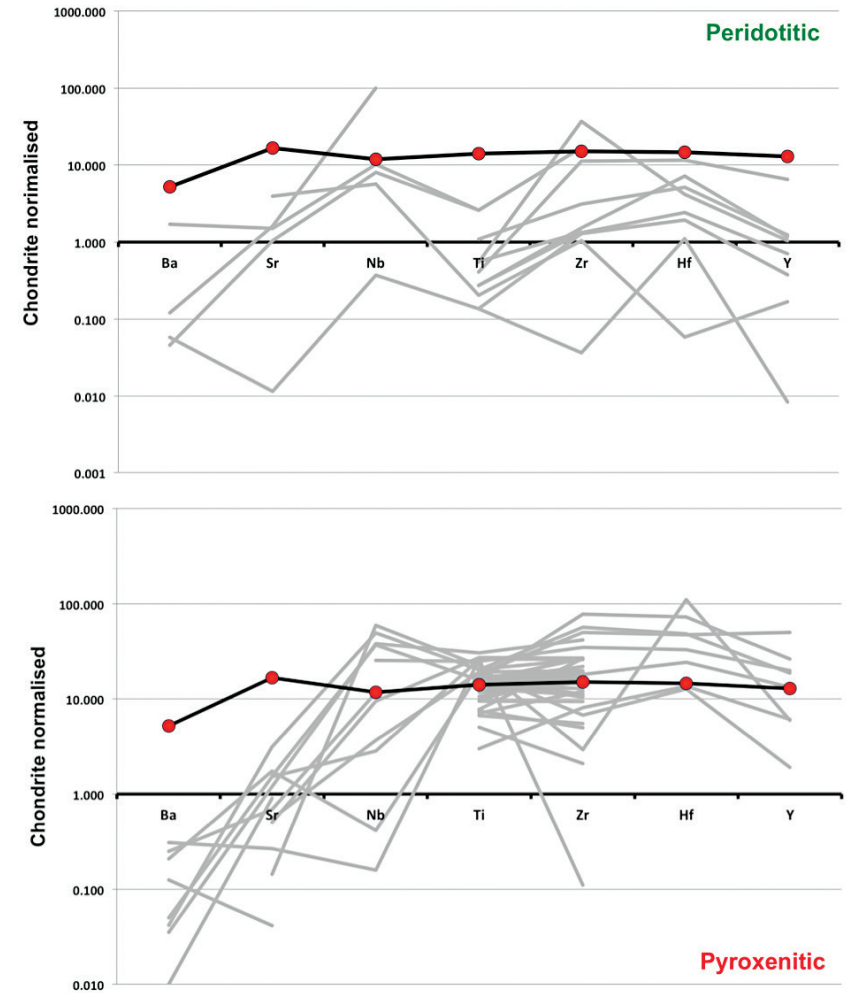


Figure S-2 Majoritic garnet LILE and HFSE abundances normalised to CI-chondrite (McDonough and Sun, 1995). Majorites of peridotitic affinity are significantly more depleted in Nb, Ti, Zr, Hf and Y than pyroxenitic majorites. Low Ba and Sr abundances in pyroxenitic majorite is possibly due to coexisting clinopyroxene. Red circles show abundances for primitive (>8.7 wt. % MgO) MORB glasses (Jenner and O'Neill, 2012).



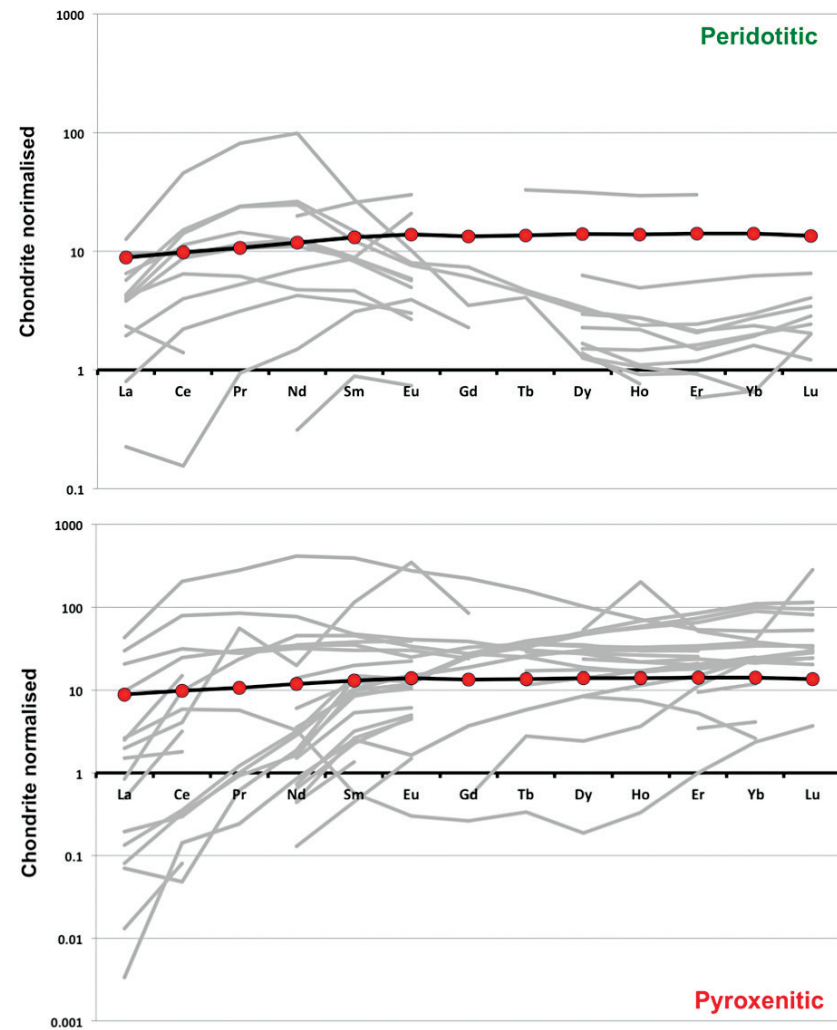


Figure S-3 Majoritic garnet REE abundances normalised to CI-chondrite (McDonough and Sun, 1995). Majorites of peridotitic affinity are significantly more depleted in Heavy REE. Red circles show abundances for primitive (>8.7 wt. % MgO) MORB glasses (Jenner and O'Neill, 2012).

Measured and calculated clinopyroxene compositions

We developed a model of Na partitioning between garnet and clinopyroxene at P of 7.5-21.5 GPa and T of 900-1700 °C using experimentally recrystallised garnet-clinopyroxene pairs from a number of experimental studies (Irifune, 1987; Yasuda *et al.*, 1994; Okamoto and Maruyama, 1998; Wang and Takahashi, 1999; Litasov and Ohtani, 2005, 2009; Bobrov *et al.*, 2008; Litasov and Ohtani, 2010; Kiseeva *et al.*, 2013). We tried several fairly complex exchange reactions, but found it difficult to improve on a simple empirical relationship fitted to the experimental data:

$$Na_{Cpx}^{6ox} = \frac{Na_{Grt}^{12ox}}{0.262 + 0.0241P - 0.00014T} \quad \text{Eq. S-1}$$

where P is in GPa and T is in K. In Equation S-1, the Na contents of clinopyroxene (Cpx) and garnet (Grt) are atomic values on 6 and 12 oxygen bases respectively. By inspection of the experimental data we see that tetrahedral Al in clinopyroxene is generally very low at these pressures, so we fixed it at 0.01 cations per formula unit. This assumption, coupled with Na partitioning leads to octahedral Al on the M1 site being Na_{Cpx}^{6ox} plus tetrahedral Al (*i.e.* $NaAlSi_2O_6$ and $CaAl_2SiO_6$ substitutions respectively). We observe that the experimental clinopyroxenes have little occupancy of the large M2 site by small cations Mg^{2+} and Fe^{2+} so we calculated the Ca content of the M2 clinopyroxene site by assuming that Na+Ca on this site is 0.95 cations per formula unit, thus allowing only 0.05 of (Mg+Fe) on M2. We then assumed that Si is 2.0 minus tetrahedral Al and that (Mg+Fe) fill the remaining M1 and M2 sites. The experimental products exhibit an approximate Fe-Mg K_d between garnet and clinopyroxene given by:

$$K_d^{Grt-Cpx} = \frac{[Fe/Mg]_{Grt}}{[Fe/Mg]_{Cpx}} \approx 2 \quad \text{Eq. S-2}$$

Equation S-2 enables us to use the garnet composition to calculate Mg/(Mg+Fe)_{Cpx}. We then have all relationships necessary to calculate the bulk clinopyroxene composition except for minor elements such as Ti, Cr and Mn. We used our model to reconstruct the compositions of clinopyroxenes in equilibrium with majoritic garnet inclusions prior to estimating a pyroxenitic bulk rock composition for the sources of the inclusions.

A number of studies have reported clinopyroxene(s) included in the same diamond as majoritic garnet (Moore and Gurney, 1989; Wilding, 1990; Hutchinson, 1997; Stachel *et al.*, 2000; Davies *et al.*, 2004; Pokhilenko *et al.*, 2004; Bulanova *et al.*, 2010). In Figure S-4 we compare calculated and reported (measured) clinopyroxene compositions for these occurrences of clinopyroxene-garnet pairs.

As can be seen, agreement between calculated and observed compositions is generally good, despite the distinct possibility that in some cases, the garnet and pyroxene were never in equilibrium with one another.



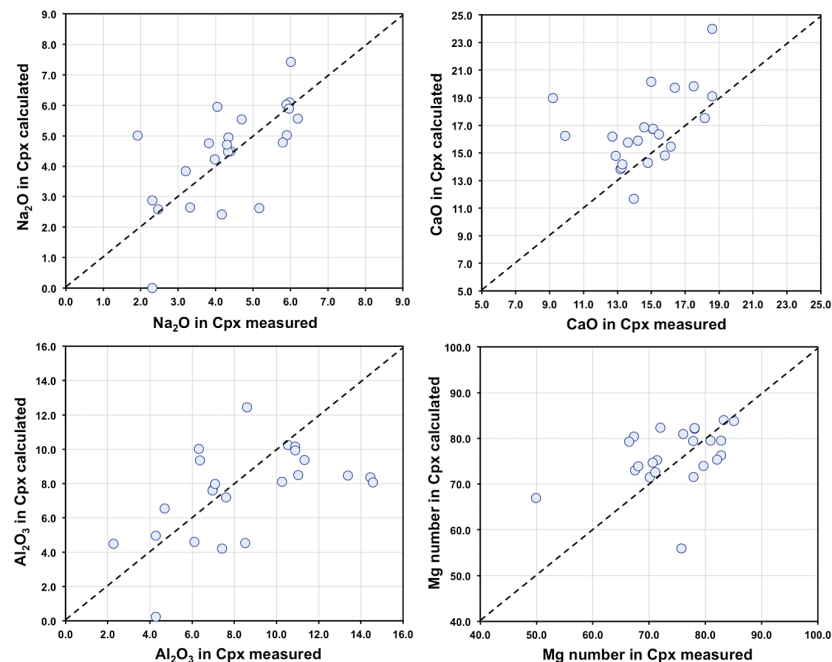


Figure S-4 Comparison of Mg#, CaO, Al₂O₃ and Na₂O contents (in wt %) of natural clinopyroxene inclusions with those calculated to be in equilibrium with pyroxenitic and eclogitic majorite. Clinopyroxene compositions are taken from the following studies: Moore and Gurney, 1989; Wilding, 1990; Hutchinson, 1997; Stachel *et al.*, 2000; Davies *et al.*, 2004; Pokhilenko *et al.*, 2004; Bulanova *et al.*, 2010.

Pressure estimates for the majoritic inclusions in diamond

Pressure was estimated using three geobarometers: by Collerson *et al.* (2010), by Beyer (2015) and by our simplified geobarometer, based on Si-content of the majorite: $P = (Si-3 + 0.11) / 0.026$, where Si is the number of Si cations in majoritic garnet per 12 oxygen formula unit.

All three geobarometers indicate that the majority of majoritic inclusions in diamond formed at pressures below 13–15 GPa, which means that they are likely in equilibrium with clinopyroxene.

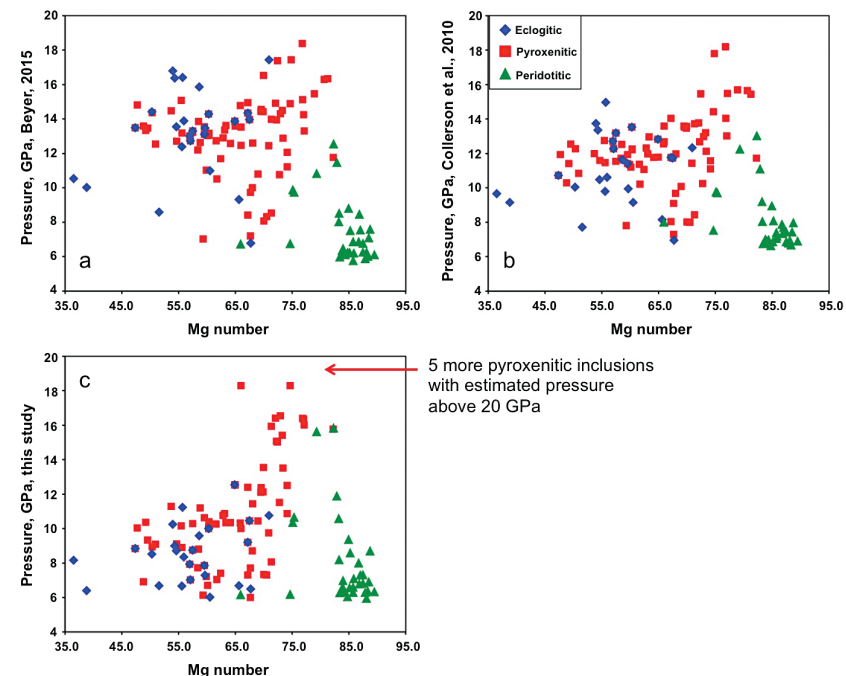


Figure S-5 Estimated pressure of majoritic inclusions based on three different geobarometers.

Experimental and analytical procedures

We performed experiments to simulate reaction across a sharp compositional boundary between peridotite and basalt (coesite-eclogite at 3 GPa), analogous to the situation in subducted lithosphere having veins and lenses of basaltic composition dispersed in peridotite (Allègre and Turcotte, 1986). Model carbonated (~5 % CaCO₃) peridotite and eclogite in the CMAS system were loaded into a Pt capsule in roughly 50/50 proportions (see Table S-1).

The experiments were performed in an end-loaded Boyd–England-type piston-cylinder apparatus at the University of Oxford. The experimental assembly consisted of a 12.7 mm O.D. calcium fluoride cylinder with inner graphite heater of 8 mm O.D and 6 mm I.D. Interior spacers were of 6 mm O.D. machineable MgO, fired at 1000 °C to ensure dryness. The 3 mm O.D. platinum capsule was surrounded and separated from the graphite furnace by a 6 mm O.D. ring of machineable MgO. The experimental pressure (3 GPa) used the calibration of McDade *et al.* (2002).



Temperature (1350 °C) was controlled and measured using a C-type ($W_{95}Re_5-W_{74}Re_{26}$) thermocouple separated from the capsule by a 0.8 mm alumina disc (Table S-1). Experiment duration was between 1.5 and 8 hours after which the run was quenched by cutting the power to the graphite heater while maintaining run pressure, which was subsequently slowly released. The recovered experimental products were mounted in acrylic resin, sectioned and hand-polished using water based lubricants and diamond pastes. We report in Table S-2 phase compositions from the longest experiment (Sa2-1) in which the reaction between eclogite and peridotite was best developed (Fig. 4 of main text).

Experiment 15-1 was carried out in a 1000-ton Walker-type multianvil device at the Institute of Geochemistry and Petrology, ETH Zürich. We used a 14/8 assembly with chromium doped MgO octahedron, stepped $LaCrO_3$ furnace and pyrophyllite gaskets. Details of assembly design and pressure calibration of the Zurich multianvil is given in Grassi and Schmidt (2011).

Table S-1 Experimental run products.

ExpN ^o	T, °C	P, GPa	Duration, h	Capsule material	Composition	Eclogite layer	Peridotite layer	Reaction zone
Sa2-1	1350	3	8	Pt	Al-rich sandwich	Grt, Co, Cor, melt	Fo, Grt, Opx, Cpx	Opx, Grt, Cpx
15-1	2150	15	2	Re	Pyroxenite			

A Re capsule was used and the pyroxenite sample (Table S-2) was held at 15 GPa and 2150 °C for 2 hours. The experiment was quenched by turning off the power supply, resulting in temperature dropping below 500 °C in less than 1 second. The recovered capsule was mounted into a low-viscosity epoxy resin ground and polished with diamond powder (1 and 3 microns diameter). Finally, polished mounts were coated with a carbon film for electron microprobe analysis.

All experimental run products were analysed using a JEOL JXA8600 electron microprobe at the Department of Archaeology at the University of Oxford. WDS analyses were conducted using a 15 kV accelerating voltage and 20 nA beam current with a focused beam of 1 micron spot in order to avoid overlapping phases. At least 50 repeat analyses were collected for each of the phases in the products. Counting times were as follows: 30 seconds peak and 15 seconds background for major elements (*e.g.*, Si, Al, Ca, Mg, Fe); 60 seconds peak and 30 seconds background for minor elements Ti, Mn, Na, K, Cr. A range of synthetic and natural standards was used for calibration. Standards for silicate glass and olivine analysis were natural wollastonite (Ca, Si), synthetic periclase (Mg), rutile (Ti), fowlerite (Mn), natural albite (Na, Al) and hematite (Fe), orthoclase (K), chromite (Cr).

Table S-2 Compositions of run products.

	SiO ₂	TiO ₂	Al ₂ O ₃	Cr ₂ O ₃	FeO	MgO	CaO	MnO	Na ₂ O	CO ₂	Sum
Sa2-1 eclogite											
Bulk	53.42		17.96			11.42	14.62			2.58	100.00
Garnet	44.46		24.90			22.88	8.78				101.01
σ	0.96		0.61			0.70	0.85				
Melt	59.49		17.49			4.53	11.36			7.15	100.01
σ	3.63		2.06			1.94	1.18				
Sa2-1 peridotite											
Bulk	45.90		4.97			41.99	4.88			2.26	100.00
Fo	42.94					58.26	0.28				101.48
σ	0.33					0.29	0.14				
Opx	57.64		4.47			37.29	2.06				101.47
σ	0.50		0.70			0.50	0.34				
Garnet	45.03		23.15			27.03	6.14				101.36
σ	1.77		2.62			2.10	0.85				
Cpx	53.31		4.40			23.58	18.39				99.68
σ	2.22		0.83			1.93	2.72				
Sa2-1 zone											
Peridotite side											
Opx	57.07		4.16			37.17	2.27				100.67
σ	1.28		0.48			0.63	0.58				
Sa2-1 zone											
Eclogite side											
Garnet	44.61		24.13			25.12	6.95				100.80
σ	0.49		1.16			2.63	1.57				
Cpx	55.06		2.62			22.84	19.41				99.93
σ	1.53		1.02			1.29	0.88				
15-1 bulk											
Garnet	48.99	0.06	11.63	0.35	6.30	20.04	11.29	0.15	1.20		100.00
Garnet	46.49	0.04	18.84	0.49	3.62	20.93	9.57	0.15	0.33		100.46
σ	0.50	0.01	0.94	0.05	0.39	0.42	0.40	0.02	0.08		
Cpx	56.07	0.04	3.13	0.22	4.25	16.31	17.04	0.11	1.50		98.66
σ	0.39	0.03	0.83	0.05	0.85	0.24	0.47	0.02	0.18		

CO₂ in melt estimated by difference.

Cpx – clinopyroxene, Opx – orthopyroxene, Grt – garnet, Fo – forsterite, Co – coesite, Cor – corundum.



Supplementary Information References

- ALLÈGRE, C.J., TURCOTTE, D.L. (1986) Implications of a 2-component marble-cake mantle. *Nature* 323, 123-127.
- BEYER, C. (2015) Geobarometry, phase relations and elasticity of eclogite under conditions of Earth's upper mantle. *PhD thesis*. University of Bayreuth, Interdisciplinary Institutions. 217pp.
- BOBROV, A.V., LITVIN, Y.A., BINDI, L., DYMSHITS, A.M. (2008) Phase relations and formation of sodium-rich majoritic garnet in the system $Mg_3Al_2Si_3O_{12}$ - $Na_2MgSi_5O_{12}$ at 7.0 and 8.5 GPa. *Contributions to Mineralogy and Petrology* 156, 243-257.
- BULANOVA, G., WALTER, M., SMITH, C., KOHN, S., ARMSTRONG, L., BLUNDY, J., GOBBO, L. (2010) Mineral inclusions in sublithospheric diamonds from Collier 4 kimberlite pipe, Juina, Brazil: subducted protoliths, carbonated melts and primary kimberlite magmatism. *Contributions to Mineralogy and Petrology* 160, 489-510.
- COLLERSON, K.D., WILLIAMS, Q., KAMBER, B.S., OMORI, S., ARAI, H., OHTANI, E. (2010) Majoritic garnet: a new approach to pressure estimation of shock events in meteorites and the encapsulation of sub-lithospheric inclusions in diamond. *Geochimica et Cosmochimica Acta* 74, 5939-5957.
- DAVIES, R.A., GRIFFIN, W.L., O'REILLY, S.Y., MCCANDLESS, T.E. (2004) Inclusions in diamonds from the K14 and K10 kimberlites, Buffalo Hills, Alberta, Canada: diamond growth in a plume? *Lithos* 77, 99-111.
- DAVIES, R.M., GRIFFIN, W.L., O'REILLY, S.Y., ANDREW, A.S. (2003) Unusual mineral inclusions and carbon isotopes of alluvial diamonds from Bingara, eastern Australia. *Lithos* 69, 51-66.
- GRASSI, D., SCHMIDT, M.W. (2011) The melting of carbonated pelites from 70 to 700km depth. *Journal of Petrology* 52, 765-789.
- HUTCHINSON, M.T. (1997) Constitution of the deep transition zone and lower mantle shown by diamonds and their inclusions. *PhD thesis*. University of Edinburgh, pp. vol. 1. 340 pp., vol. 2. 306 pp.
- IRIFUNE, T. (1987) An experimental investigation of the pyroxene garnet transformation in a pyrolite composition and its bearing on the constitution of the mantle. *Physics of The Earth and Planetary Interiors* 45, 324-336.
- JENNER, F.E., O'NEILL, H.S. (2012) Analysis of 60 elements in 616 ocean floor basaltic glasses. *Geochemistry Geophysics Geosystems* 13.
- KAMINSKY, F.V., ZAKHARCHENKO, O.D., DAVIES, R., GRIFFIN, W.L., KHACHATRYAN-BLINOVA, G.K., SHIRYAEV, A.A. (2001) Superdeep diamonds from the Juina area, Mato Grosso State, Brazil. *Contributions to Mineralogy and Petrology* 140, 734-753.
- KISEEVA, E.S., LITASOV, K.D., YAXLEY, G.M., OHTANI, E., KAMENETSKY, V.S. (2013) Melting and phase relations of carbonated eclogite at 9–21 GPa and the petrogenesis of alkali-rich melts in the deep mantle. *Journal of Petrology* 54, 1555-1583.
- LITASOV, K.D., OHTANI, E. (2005) Phase relations in hydrous MORB at 18-28 GPa: implications for heterogeneity of the lower mantle. *Physics of the Earth and Planetary Interiors* 150, 239-263.
- LITASOV, K.D., OHTANI, E. (2009) Solidus and phase relations of carbonated peridotite in the system CaO - Al_2O_3 - MgO - SiO_2 - Na_2O - CO_2 to the lower mantle depths. *Physics of the Earth and Planetary Interiors* 177, 46-58.
- LITASOV, K., OHTANI, E. (2010) The solidus of carbonated eclogite in the system CaO - Al_2O_3 - MgO - SiO_2 - Na_2O - CO_2 to 32 GPa and carbonatite liquid in the deep mantle. *Earth and Planetary Science Letters* 295, 115-126.
- MCDADE, P., WOOD, B.J., VAN WESTRENNEN, W., BROOKER, R., GUDMUNDSSON, G., SOULARD, H., NAJORKA, J., BLUNDY, J. (2002) Pressure corrections for a selection of piston-cylinder cell assemblies. *Mineralogical Magazine* 66, 1021-1028.
- MCDONOUGH, W.F., SUN, S.S. (1995) The Composition of the Earth. *Chemical Geology* 120, 223-253.



- MOORE, R.O., GURNEY, J.J. (1989) Mineral inclusions in diamond from Monastery kimberlite, South Africa, in: Ross et al. (Editors), *Kimberlites and related rocks, Proceedings of the IVth International Kimberlite Conference*. Blackwell, Carlton, Perth, pp. 1029-1041.
- MOORE, R.O., GURNEY, J.J., GRIFFIN, W.L., SHIMIZU, N., 1991. ULTRA-HIGH PRESSURE GARNET INCLUSIONS IN MONASTERY DIAMONDS: TRACE ELEMENT ABUNDANCE PATTERNS AND CONDITIONS OF ORIGIN. *EUROPEAN JOURNAL OF MINERALOGY* 3, 213-230.
- OKAMOTO, K., MARUYAMA, S. (1998) Multi-anvil re-equilibration experiments of a Dabie Shan ultrahigh-pressure eclogite within the diamond-stability fields. *The Island Arc* 7, 52-69.
- POKHILENKO, N.P., SOBOLEV, N.V., McDONALD, J.A., HALL, A.E., YEFIMOVA, E.S., ZEDGENIZOV, D.A., LOGVINOVA, A.M., REIMERS, L.F. (2001) Crystalline inclusions in diamonds from kimberlites of the Snap Lake area (Slave Craton, Canada): new evidences for the anomalous lithospheric structure. *Doklady Earth Sciences* 380, 806-811.
- POKHILENKO, N.P., SOBOLEV, N.V., REUTSKY, V.N., HALL, A.E., TAYLOR, L.A. (2004) Crystalline inclusions and C isotope ratios in diamonds from the Snap Lake/King Lake kimberlite dyke system: evidence of ultradeep and enriched lithospheric mantle. *Lithos* 77, 57-67.
- STACHEL, T., HARRIS, J.W. (1997) Diamond precipitation and mantle metasomatism - evidence from the trace element chemistry of silicate inclusions in diamonds from Akwatia, Ghana. *Contributions to Mineralogy and Petrology* 129, 143-154.
- STACHEL, T., HARRIS, J.W., BREY, G.P. (1998a) Rare and unusual mineral inclusions in diamonds from Mwadui, Tanzania. *Contributions to Mineralogy and Petrology* 132, 34-47.
- STACHEL, T., VIJJOEN, K.S., BREY, G., HARRIS, J.W. (1998b) Metasomatic processes in Iherzolitic and harzburgitic domains of diamondiferous lithospheric mantle: REE in garnets from xenoliths and inclusions in diamonds. *Earth and Planetary Science Letters* 159, 1-12.
- STACHEL, T., BREY, G.P., HARRIS, J.W. (2000) Kankan diamonds (Guinea) I: from the lithosphere down to the transition zone. *Contributions to Mineralogy and Petrology* 140, 1-15.
- TAPPERT, R., STACHEL, T., HARRIS, J.W., MUEHLENBACHS, K., LUDWIG, T., BREY, G.P. (2005) Diamonds from Jagersfontein (South Africa): messengers from the sublithospheric mantle. *Contributions to Mineralogy and Petrology* 150, 505-522.
- WANG, W.Y., SUENO, S., TAKAHASHI, E., YURIMOTO, H., GASPARIK, T. (2000) Enrichment processes at the base of the Archean lithospheric mantle: observations from trace element characteristics of pyrope garnet inclusions in diamonds. *Contributions to Mineralogy and Petrology* 139, 720-733.
- WANG, W.Y., TAKAHASHI, E. (1999) Subsolvus and melting experiments of a K-rich basaltic composition to 27 GPa: implication for the behavior of potassium in the mantle. *American Mineralogist* 84, 357-361.
- WILDING, M.C. (1990) A study of diamonds with syngenetic inclusions. *PhD thesis*. University of Edinburgh, p. 281.
- YASUDA, A., FUJII, T., KURITA, K. (1994) Melting phase relations of an anhydrous mid-ocean ridge basalt from 3 to 20 GPa: implications for the behavior of subducted oceanic crust in the mantle. *Journal of Geophysical Research-Solid Earth* 99, 9401-9414.

